Stereospecific Synthesis of a Carbene-Generating Angiotensin II Analogue for Comparative Photoaffinity Labeling: Improved Incorporation and Absence of Methionine Selectivity

Dany Fillion, Maud Deraët, Brian J. Holleran, and Emanuel Escher*

Department of Pharmacology, Faculté de Médecine et des Sciences de la Santé, Université de Sherbrooke, Sherbrooke, Québec, Canada J1H 5N4

Received September 26, 2005

A stereospecific convergent synthesis of *N*-[(9-fluorenyl)methoxycarbonyl]-*p*-[3-(trifluoromethyl)-3*H*-diazirin-3-yl]-L-phenylalanine (Fmoc-**12**, Fmoc-Tdf) and its incorporation into the C-terminal position of the angiotensin II (AngII) peptide to form ^{125}I[Sar^1,Tdf^8]AngII (^{125}I-**13**) is presented. This amino acid photoprobe is a highly reactive carbene-generating diazirine phenylalanine derivative that can be used for photoaffinity labeling. Using model receptors, we compared the reactivity and the Met selectivity of **12** to that of the widely used and reputedly Met-selective *p*-benzoyl-L-phenylalanine (Bpa) photoprobe. Wild-type and mutant AngII type 2 receptors, a G protein-coupled receptors, were photolabeled with ^{125}I-**13** as well as with ^{125}I-[Sar^1,Bpa^8]AngII (^{125}I-**14**), and the respective incorporation yields were assessed. The carbene-generating **12** was more reactive toward inert residues and was not Met-selective compared to the biradical ketone-generating Bpa, allowing for more precise determination of ligand contact points in peptidergic receptors.

Introduction

G protein-coupled receptors (GPCRs), also known as heptahelical receptors, are the largest family of cell surface receptors mediating multiple responses to a large variety of hormonal and sensory signals.[1] As common characteristic, GPCRs possess seven transmembrane domains (TMDs) that constitute the structural scaffold of these transmembrane proteins. Elucidating the mechanisms by which GPCRs carry out their biological functions requires a detailed molecular understanding of ligand−receptor interactions leading to receptor activation and signal transduction. The most widely used methods to probe receptor structures include classic structure−activity relationships, computational molecular modeling, site-directed mutagenesis, magnetic resonance spectroscopies, X-ray crystallography, and direct labeling methods such as photoaffinity labeling.[2,3] Over the past three decades, photoaffinity labeling has emerged as an important biochemical method for the direct mapping of peptide−protein interactions.[4−7] Following the binding of the photoreactive ligand within its cognate receptor, the photoprobe is photoactivated by its conversion into a highly reactive intermediate that causes covalent bonding within its immediate molecular surroundings, presumably at its contact area within the receptor. This method provides an insight into dynamic systems under physiological conditions by making it possible to analyze the exact incorporation locus of the photoprobe in the receptor. This information may then be used in conjunction with techniques such as computational molecular modeling procedures[8,9] to design and validate molecular models of liganded receptors. Several recent reviews on the applications of photoaffinity labeling for drug discovery and development highlight this trend.[10−12]

Most photoaffinity labeling studies of peptidergic GPCRs have been conducted with photoprobes containing the benzophenone moiety within the phenylalanine derivative *p*-benzoyl-L-phenylalanine (Bpa).[13−15] However, Bpa has two important drawbacks. First, the bulky size of the benzophenone moiety may interfere with the ligand recognition site and/or the biological activity of the target protein. For instance, [Sar^1,-Bpa^8]AngII (**14**), where Bpa is introduced instead of the native Phe in the C-terminal position of the peptide, is a neutral antagonist of the human angiotensin II (AngII) type 1 receptor (hAT_1),[16] whereas native AngII is a full agonist. This may reduce the usefulness of Bpa in the analysis of the conformational changes associated with receptor activation. Second, previous studies by us and others have shown that Bpa has a pronounced selectivity for Met residues in receptors.[17−22] This reduces the precision of the photolabeling since Bpa may selectively photolabel more distant Met residues instead of the nearest non-Met residues. We recently exploited this unique Met selectivity of Bpa to introduce a new method, the methionine proximity assay (MPA), for scanning the contact areas of peptidergic GPCRs and confirming suspected peptide−GPCR contact points.[22,23]

To circumvent the selective photolabeling properties of Bpa, alternative photolabeling chemical groups with different photochemical properties have to be used.[24] These include nitrene-producing arylazides and carbene-producing aryldiazirines. Nonsubstituted arylnitrene groups, however, undergo an intramolecular rearrangement leading to an electrophilic cyclic ketenimine intermediate that may react with distant nucleophiles due to its relatively long lifespan.[25] Trifluoromethylaryldiazirine groups have been reported to generate highly reactive carbenes that react with virtually all 20 amino acids with no intramolecular rearrangements.[26] However, the challenging, time-consuming synthesis of the phenylalanine derivative *p*-[3-(trifluoromethyl)-3*H*-diazirin-3-yl]-L-phenylalanine (**12**, Tdf)[27−30] has until now prevented more widespread use of this photoprobe.

We present herein a new stereospecific convergent synthesis procedure for *N*-[(9-fluorenyl)methoxycarbonyl]-*p*-[3-(trifluoromethyl)-3*H*-diazirin-3-yl]-L-phenylalanine (Fmoc-**12**, Fmoc-Tdf), its incorporation into the C-terminal position of the AngII peptide, and the radioiodination of the resulting peptide to form ^{125}I[Sar^1,Tdf^8]AngII (^{125}I-**13**). To investigate the photolabeling properties of the diazirine analogue ^{125}I-**13** and the benzophenone analogue ^{125}I-**14**, we assessed the respective incorporation yields on the wild-type (wt) and mutant AngII type 2 model receptor (AT_2) of human origin (hAT_2). Previous studies demonstrated that ^{125}I-**14** simultaneously photolabels Met128

* To whom correspondence should be addressed. Phone: (819) 564-5346. Fax: (819) 564-5400. E-mail: Emanuel.Escher@USherbrooke.ca.

10.1021/jm050958a CCC: $33.50
Published on Web 03/15/2006

Scheme 1. Tdf Synthesis[a]

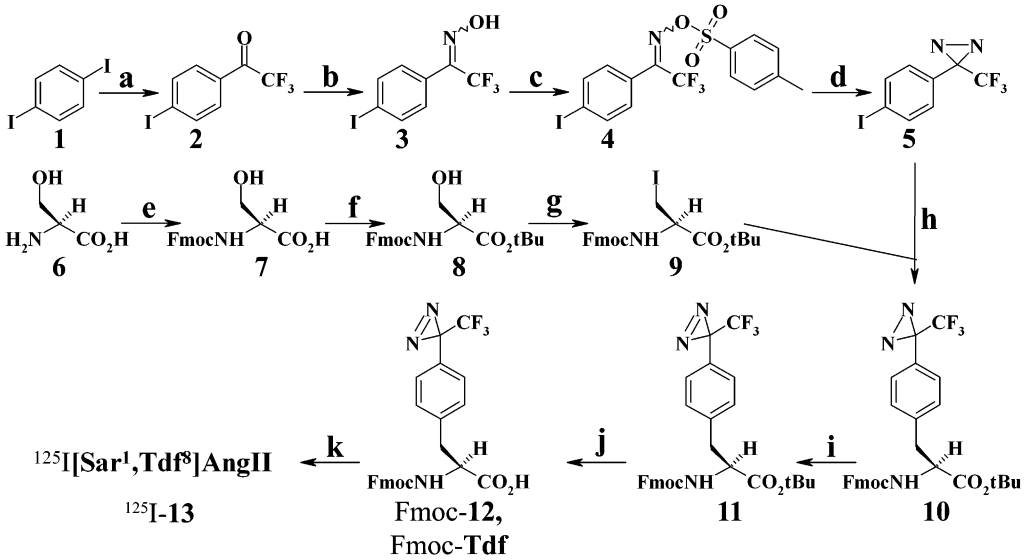

[a] Reagents and conditions: (a) *n*-BuLi, CF_3CO_2Et, Et_2O, 4 h, −78 °C/rt, 81%; (b) $NH_2OH{\cdot}HCl$, EtOH, Pyr, 2 h, reflux, 94%; (c) TsCl, Pyr, 2 h, reflux, 94%; (d) NH_3, ET_2O, 12−16 h, −78 °C/rt, 96%; (e) Fmoc-OSu/1,4-dioxane, Na_2CO_3/H_2O, 24 h, 0 °C/rt, 92%; (f) DCC, *t*-BuOH, Cu(I)Cl, CH_2Cl_2, 74 h, rt, 67%; (g) $Me(PhO)_3PI$, *N*,*N*-DMF, 1 h, rt, 88% or $ClPh_2P$, imidazole, I_2, CH_2Cl_2, 1 h, 53%; (h) Zn*, $Pd_2(dba)_3$, P(*o*-tol)$_3$, *N*,*N*-DMF, 3 h, rt, 55%; (i) Ag_2O, ET_2O, 8 h, rt, 87%; (j) CF_3CO_2H, Et_3Si, CH_2Cl_2, 3 h, rt, 81%; (k) SPPS using Wang resin, $Na^{125}I$, IODO-GEN iodination reagent (1,3,4,6-tetrachloro-3α,6α-diphenylglycoluril), 1500 Ci/mmol.

and Met138 within TDM3 on the hAT_2-wt receptor.[22,31] This unique methionine environment makes AT_2 an ideal model system in which to compare reactivity and Met selectivity of photoprobes. The AT_2 receptor is a glycosylated[32] peptidergic GPCR of 363 amino acids with a protein-only molecular mass of 41 kDA and whose pharmacological and physiological functions are still somewhat controversial.[33−36]

Chemistry

Others have reported the synthesis of **12**. One approach involves the alkylation of a glycine derivative with *p*-[3-(trifluoromethyl)-3-aryldiazirine]benzyl halide under basic conditions followed by a wasteful enzymatic resolution of the *N*-acyl amino acid.[27,28] A second approach uses a noncommercial Ni complex chiral auxiliary.[29,30] We report here the stereospecific convergent synthesis of Fmoc-**12** using commercial *p*-diiodobenzene (**1**) and L-serine (**6**) as starting materials. The key step is a palladium-catalyzed coupling reaction of a *p*-diaziridinyliodoaryl derivative (**5**) with an orthogonally diprotected *β*-iodoalanine organozinc reagent (Zn-**9**). Fmoc-**12** was incorporated into the C-terminal position of AngII, which was radioiodinated to form radiophotoreactive ^{125}I-**13** (Scheme 1).

The photoreactive moiety of **12**, compound **5**, was synthesized in four steps according to the literature.[37,38] Compound **1** was converted into ketone **2** in good yields by reacting the corresponding organolithium salt with ethyl α,α,α-trifluoroacetate and was used without further purification.[37] Attempts to synthesize **2** by reacting the organolithium reagent with α,α,α-trifluoroacetic anhydride resulted in poor yield. Reacting **2** with hydroxylamine hydrochloride yielded the corresponding oxime **3**,[38] which was subsequently, without further purification, converted into the corresponding tosyl oxime **4** in high yields through a reaction with *p*-toluenesulfonyl chloride.[38,39] Mesylation of **4** has been reported to be superior to tosylation since fewer byproducts are formed.[40] In the present study, the two methods provided equivalent results. The direct reaction of **2** with hydroxylamine tosyl oxime is an alternative method for synthesizing **4**. Reacting **4** with ammonia at high pressure generated a high yield of the corresponding pure *p*-diaziridinyliodoaryl **5**.[38] When done at atmospheric pressure, this step resulted in lower yields.

The chiral moiety of **12**, compound **6**, was orthogonally diprotected and iodinated prior to the palladium-catalyzed coupling reaction with **5**. Protecting the NH_2 group of **6** with *N*-[(9-fluorenyl)methoxycarbonyloxy]succinimide resulted in a high yield of monoprotected amino acid **7**, which was used without further purification.[41] Subsequent protection of the CO_2H group of **7** using a mixture of dicyclohexylcarbodiimine, *tert*-butyl alcohol, and copper(I) chloride generated a high yield of diprotected amino acid **8**.[42] In our hands, this *tert*-butylation method was the least expensive and most effective. Compound **8** was iodinated to form diprotected *β*-iodoalanine **9** through a reaction with either methyltriphenoxyphosphonium iodide[43] or a mixture of chlorodiphenylphosphine, imidazole, and iodine,[44] which resulted in high to moderate yields, respectively.

The key step of this synthesis procedure was the palladium-catalyzed coupling reaction of the *p*-diaziridinyliodoaryl derivative **5** with the diprotected *β*-iodoalanine-derived zinc reagent Zn-**9**. Compound **5** was coupled to **9** in a moderate yield reaction using activated Zn* and tris(dibenzylideneacetone)dipalladium-(0)/tri-*o*-tolylphosphine catalyst to generate the diprotected phenylalanine diaziridine **10**.[45] Oxidation of **10** using silver oxide generated a high yield of diprotected phenylalanine diazirine **11**.[38,39] Last, deprotection of the CO_2H group of **11** using a mixture of α,α,α-trifluoroacetic acid and triethylsilane resulted in a good yield of Fmoc-**12**.[45]

Fmoc-**12** was incorporated into AngII by esterification to hydroxyl-Wang resin, followed by chain elongation by standard solid-phase peptide synthesis using the Fmoc/piperidine procedure.[46] The resulting photoreactive **13** was radioiodinated[47] to form radiophotoreactive ^{125}I-**13** with a specific activity of approximately 1500 Ci/mmol.

Results and Discussion

The precision of the photolabeling process may be reduced considerably if chemical selectivity of the photoprobe is present. Selective photoprobes may photolabel distant reactive residues instead of inert residues in their immediate surroundings. The

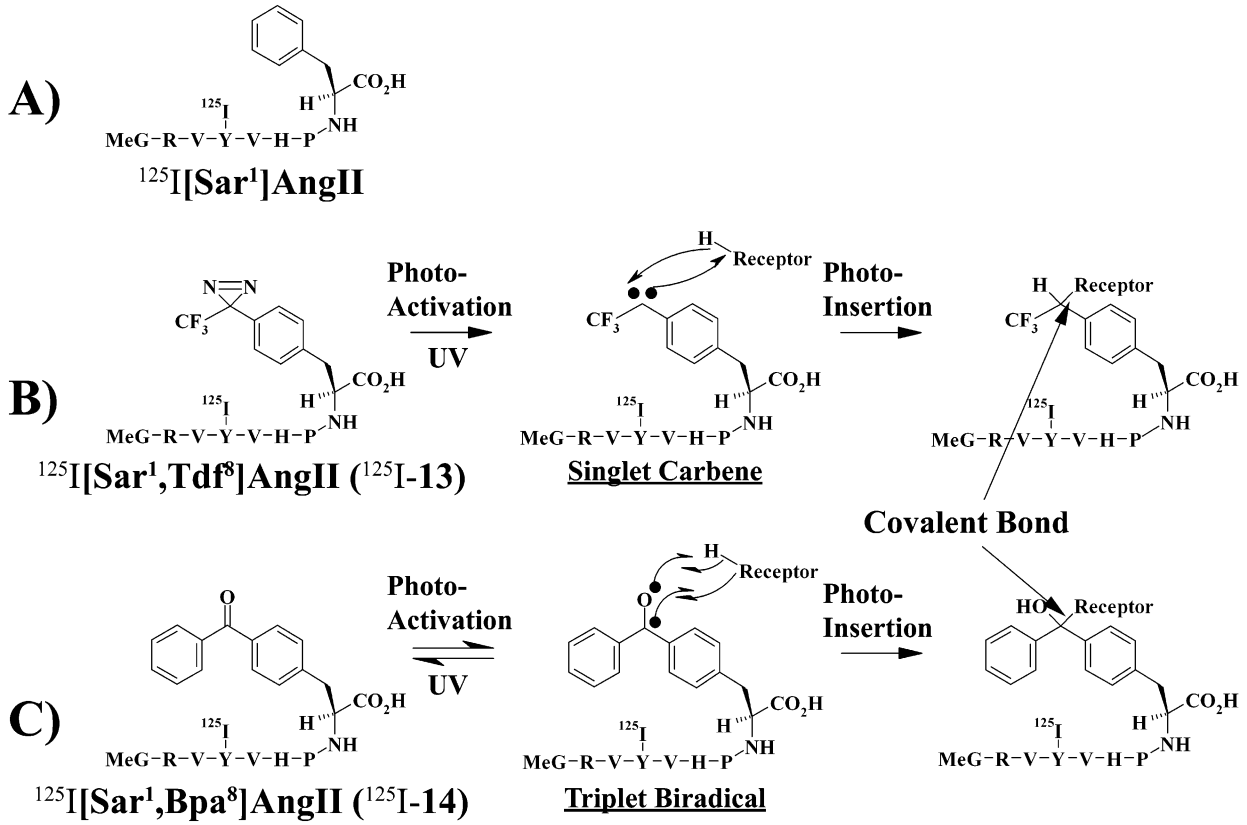

Figure 1. Amino acid sequence and photochemistry of (A) native AngII, (B) ^{125}I-**13**, and (C) ^{125}I-**14**. The photogenerated carbene of **13** is an electrophilic electron-deficient sextet species displaying irreversible photoactivation to the singlet state.[13−15] The photogenerated biradical ketone of Bpa is an electrophilic electronic transition from an oxygen nonbonding sp^2-like n-orbital to a carbonyl group antibonding π^*-orbital displaying reversible photoactivation to the triplet state.[26−28]

present study was thus undertaken to evaluate the Met selectivity and reactivity of carbene-generating **12** compared to the widely used biradical ketone-generating Bpa, two amino acid photoprobes (Figure 1).

To investigate the reactivity and Met selectivity of diazirine analogue ^{125}I-**13** and benzophenone analogue ^{125}I-**14**, several hAT_2 mutant receptors were constructed. The endogenous Met128 and Met138 residues in TMD3, the previously determined contacts of the C-terminal amino acid for ^{125}I-**14** in the hAT_2 receptor,[22,31] were replaced either one by one or simultaneously by Ala residues or by more isosteric Leu residues (Figure 2). The pharmacological parameters describing the equilibrium binding to wild-type and mutant receptors of both ^{125}I-**13** and ^{125}I-**14** were compared. Both AngII analogues had practically identical high binding affinities (K_d) on the wild-type and mutant hAT_2 receptors that were comparable to those of the AngII peptide (Table 1). All the mutant receptors had maximum binding capabilities (B_{max}) that were similar to that of the wild-type receptor. We were thus able to directly compare the incorporation yields of these model receptors using both AngII analogues. In general, replacing Met residues by hydrophobic Leu or Ala residues in helical TMDs does not perturb the global conformation of the mutant protein and is of little consequence to overall receptor properties and hence ligand interactions.[48]

To ensure that the diazirine analogue ^{125}I-**13** photolabeled the same hAT_2 receptor regions as the benzophenone analogue ^{125}I-**14**, the hAT_2-wt receptor and the isosteric hAT_2-M128,-138L double-mutant receptor were photolabeled with both AngII analogues and were then subjected to CNBr cleavage, a C-terminal Met-specific reagent (Figure 3). The SDS−PAGE CNBr cleavage patterns were identical, indicating that both ^{125}I-**13** and ^{125}I-**14** photolabeled the fragment containing Met128 and Met138 within TMD3 of the hAT_2 receptor. Photolabeled Met residues are resistant to CNBr cleavage when labeled on the γ-methylene[49] and undergo slower cleavage but release a methyl isothiocyanate derivative of the photoprobe when labeled at the ϵ-methyl group.[17] The CNBr cleavage of the hAT_2-wt receptor photolabeled with both AngII analogues produced, for the benzophenone analogue ^{125}I-**14**, fragment Phe129−Met170 with the photoprobe attached to Met138 (lane 3, apparent molecular mass 6.2 kDa, expected molecular mass 6.1 kDa), fragment Cys117−Met138 with the photoprobe attached to Met128 (lane 3, apparent molecular mass 4.2 kDa, expected molecular mass 3.5 kDa), and the released photoprobe (lane 3, apparent molecular mass less than 3.4 kDa, expected molecular mass 1.1 kDa). The same fragments were also observed with the diazirine analogue ^{125}I-**13**, that is, Phe129−Met170 (lane 5, apparent molecular mass 6.2 kDa, expected molecular mass 6.1 kDa), fragment Cys117−Met138 (lane 5, apparent molecular mass 4.2 kDa, expected molecular mass 3.5 kDa), and also the released photoprobe (lane 5, apparent molecular mass below 3.4 kDa, expected molecular mass 1.1 kDa), but to a lower degree than with the ^{125}I-**14** photolabeled receptor. The insertion of ^{125}I-**13** within the sequence Phe129−Met138 would result in a 2.2 kDa fragment, which appeared to be present (lane 5). Finally, the CNBr cleavage of the hAT_2-M128,138L double-mutant receptor photolabeled with both AngII analogues produced a single large fragment, Cys117−Met170 (lanes 4 and 6, apparent molecular mass 6.4 kDa, expected molecular mass 7.4 kDa), but no smaller fragments.

To assess the Met selectivity and reactivity of **12** and Bpa, quantitative photoaffinity labeling experiments were performed using the model receptors (Figure 4 and Table 2). Met selectivity

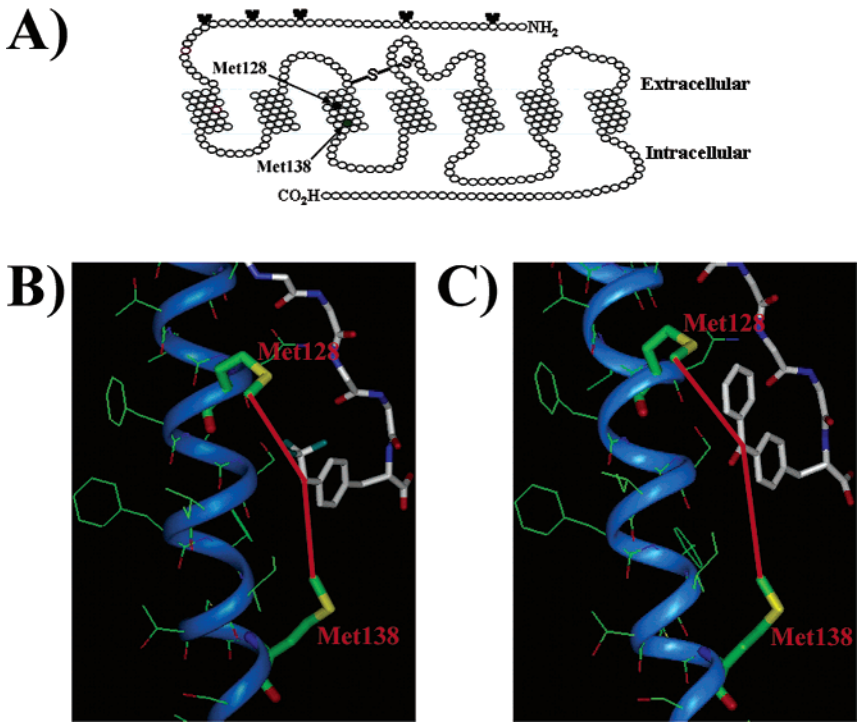

Figure 2. (A) 2D schematic representation of the primary structure of the hAT_2 receptor. Endogenous Met128 and Met138, which were mutated for Leu and Ala, are represented. Putative sites of N-glycosylation on Asn4, Asn13, Asn24, Asn29, and Asn34 are also indicated. Rhodopsin-homology molecular modeling according to Rihakova et *al.*[22] showing the endogenous Met128 and Met138 residues in TMD3 interacting with both photoactivated AngII analogues: (B) ^{125}I-**13**; (C) ^{125}I-**14**.

Table 1. Pharmacological Parameters of the Wild-Type and Mutant hAT_2 Receptors[a]

	K_d (nM)			B_{max}
	^{125}I-**13**	^{125}I-**14**	AngII	(pmol/mg)
hAT_2-wt	2.1 ± 0.3	2.3 ± 0.3	0.21 ± 0.02	5.2 ± 0.5
hAT_2-M128L	1.1 ± 0.1	1.2 ± 0.1	0.30 ± 0.03	3.8 ± 0.4
hAT_2-M138L	1.2 ± 0.1	1.1 ± 0.1	0.32 ± 0.03	6.9 ± 0.6
hAT_2-M128,138L	1.2 ± 0.1	1.2 ± 0.1	0.13 ± 0.01	5.2 ± 0.4
hAT_2-M128A	1.2 ± 0.1	1.1 ± 0.1	0.11 ± 0.01	3.0 ± 0.3
hAT_2-M138A	1.1 ± 0.1	1.2 ± 0.1	0.25 ± 0.02	6.5 ± 0.5
hAT_2-M128,138A	1.2 ± 0.1	1.2 ± 0.1	0.30 ± 0.03	1.8 ± 0.2

[a] See the Experimental Section for details. Affinities (K_d) are presented in nM, and maximum binding capacities (B_{max}; established with ^{125}I-**13**) are presented in pmol/mg of protein in the sample. The means ± SE are shown for three independent experiments, each with duplicate determinations.

could be quantified if a significant reduction in incorporation occurred on the hAT_2-M128,138L double-mutant receptor compared to the hAT_2-wt receptor. The benzophenone analogue ^{125}I-**14** resulted in a 57% incorporation yield with the hAT_2-wt receptor compared to 5% with the M → L double-mutant receptor. The diazirine analogue ^{125}I-**13** photolabeled the hAT_2-wt receptor and the M → L double-mutant receptor with similar efficiencies of 24% and 21%, respectively. Both AngII analogues photolabeled the single-mutant hAT_2-M128L, hAT_2-M138L, hAT_2-M128A, and hAT_2-M138A receptors to the same extent. The incorporation yields of the single mutants were similar to that of the hAT_2-wt receptor, although yields of the M → A single-mutant receptors tended to be lower, but remained well within the range of the M → L single-mutant receptors. The higher reactivy of **12** over biradical-generating Bpa could also be evidenced on the basis of their photolabeling efficiencies with respect to the hAT_2-M138,138A double-mutant receptor. An incorporation yield of 6% was observed for ^{125}I-**13** compared to less than 1% for ^{125}I-**14**.

Incorporation yield time-course experiments with both AngII analogues on the hAT_2-wt and the hAT_2-M128,138L double-mutant receptors revealed that the incorporation yield was optimal after 15 min of irradiation for the diazirine analogue ^{125}I-**13**, but needed to be extended up to 60 min for the benzophenone analogue ^{125}I-**14** (Figure 5). Diazirine photolysis is irreversible and photodissociative, leading to the loss of N_2 and the generation of carbene. In contrast, benzophenone photolysis is reversible and may involve many excitation−relaxation cycles until a favorable conformation for covalent bonding is achieved. Indeed, prolonged irradiation appears to increase the incorporation yield. Benzophenone-photolabeled proteins do not necessarily reflect the principal incorporation locus of the photoprobe since the repetitive nature of photoactivation together with the Met selectivity may result in the predominant photolabeling of less preferred conformations and, consequently, skewed conclusions.

These results show, on one hand that, unlike Bpa, carbene-generating **12** is not Met-selective. The benzophenone analogue ^{125}I-**14** has a greater than 10-fold preference of incorporation for Met residues on the hAT_2-wt receptor compared to Leu residues on the hAT_2-M128,138L double-mutant receptor, whereas the diazirine analogue ^{125}I-**13** has the same incorporation efficiency with both receptors. On the other hand, the fact that ^{125}I-**13** has a 4−6-fold higher photolabeling efficiency than ^{125}I-**14** with the hAT_2-M128,138L and hAT_2-M128,138A double-mutant receptors indicates that **12** was much more reactive toward non-Met residues than Bpa. The hAT_2-M128,138A double-mutant receptor reduces the close van der Waals contact between the C-terminal position of AngII and the hAT_2 receptor in this unique microenvironment only and not elsewere. Some studies have reported that Bpa may have an incorporation yield of up to 90% of the specific binding capacity of the target protein.[14] These high incorporation yields may be due to the intrinsically more reactive residues in the target protein and/or

Table 2. Incorporation Yields of ^{125}I-**13** and ^{125}I-**14** on Model Receptors[a]

	incorporation yield (%)			incorporation yield (%)	
	^{125}I-**13**	^{125}I-**14**		^{125}I-**13**	^{125}I-**14**
hAT_2-wt	24 ± 2	57 ± 6	hAT_2-M138L	24 ± 2	49 ± 5
hAT_2-M128,138L	21 ± 2	5 ± 1	hAT_2-M128A	19 ± 2	41 ± 4
hAT_2-M128,138A	6 ± 1	<1 ± 1	hAT_2-M138A	20 ± 2	43 ± 4
hAT_2-M128L	22 ± 2	46 ± 5			

[a] See the Experimental Section for details. Each AngII analogue−hAT_2 receptor interaction was specific and decreased in a dose-dependent manner in the presence of AngII (results not shown). The means ± SE are shown for five independent experiments.

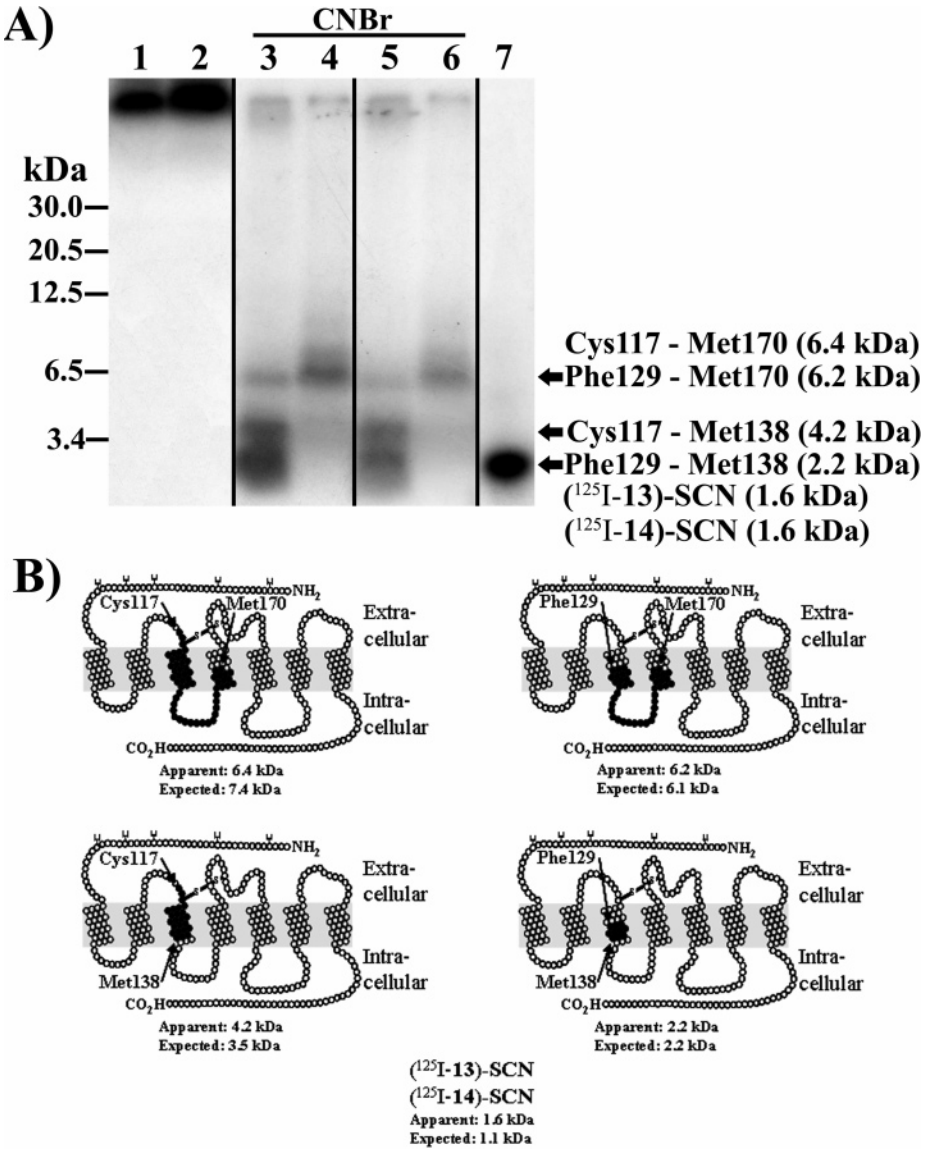

Figure 3. (A) SDS−PAGE autoradiography after C-terminal Met-specific CNBr cleavage of the photolabeled ^{125}I-**13**/hAT_2 and ^{125}I-**14**/hAT_2 complexes. hAT_2-wt receptor and isosteric hAT_2-M128,138L double-mutant receptor transfected cell membranes were photolabeled with either ^{125}I-**13** or ^{125}I-**14**, solubilized, partially purified, and submitted to CNBr cleavage. The CNBr cleavage pattern was analyzed by 16.5% T/3% C Tris−Tricine/SDS−PAGE followed by autoradiography (see the Experimental Section for details). Key: lane 1, ^{125}I-**14**/hAT_2-wt − CNBr; lane 2, ^{125}I-**13**/hAT_2-wt − CNBr; lane 3, ^{125}I-**14**/hAT_2-wt + CNBr; lane 4, ^{125}I-**14**/hAT_2-M128,138L + CNBr; lane 5, ^{125}I-**13**/hAT_2-wt + CNBr; lane 6, ^{125}I-**13**/hAT_2-M128,138L + CNBr; lane 7, ^{125}I-**14** and ^{125}I-**13**. ^{14}C-labeled low molecular mass protein standards were run in parallel. Each AngII analogue−hAT_2 receptor interaction was specific and decreased in a dose-dependent manner in the presence of AngII (results not shown). This figure is representative of four independent experiments. (B) 2D schematic representation of the primary structure of the hAT_2 receptor showing the CNBr-generated fragments in black closed circles.

to its Met selectivity. Several reports have also demonstrated that the 3-(trifluoromethyl)-3-aryldiazirine group has comparable photolabeling properties, but it is not widely used due to its difficult synthetic access.[6,7,12,50−54]

The photochemical basis of the Met selectivity of benzophenone-containing Bpa has already been studied.[55−57] Met-containing peptides quench the triplet biradical ketone of the excited benzophenone via a charge-transfer complex at the sulfur atom. This mechanism seems to be effective when nonbonding electron pairs of heteroatoms are proximal to the triplet biradical ketone.[14,15] Incorporation yields in Met are increased since this electron transfer is more than 10^4-fold quicker than toward Ala residues. Indeed, photolabeling by Bpa of the double-Met environment in the hAT_2-wt receptor resulted in the highest

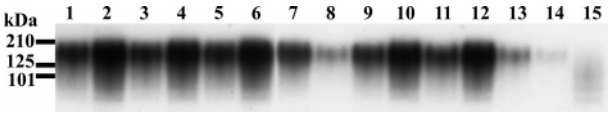

Figure 4. SDS−PAGE autoradiography showing the incorporation yields of both ^{125}I-**13** and ^{125}I-**14** in the glycosylated hAT_2 receptor. Receptor-transfected cell membranes were photolabeled with either ^{125}I-**13** or ^{125}I-**14**, solubilized, and analyzed by 7.5% Tris−glycine/SDS−PAGE followed by autoradiography (see the Experimental Section for details). Key: lane 1, ^{125}I-**13**/hAT_2-wt; lane 2, ^{125}I-**14**/hAT_2-wt; lane 3, ^{125}I-**13**/hAT_2-M128L; lane 4, ^{125}I-**14**/hAT_2-M128L; lane 5, ^{125}I-**13**/hAT_2-M138L; lane 6, ^{125}I-**14**/hAT_2-M138L; lane 7, ^{125}I-**13**/hAT_2-M128,-138L; lane 8, ^{125}I-**14**/hAT_2-M128,138L; lane 9, ^{125}I-**13**/hAT_2-M128A; lane 10, ^{125}I-**14**/hAT_2-M128A; lane 11, ^{125}I-**13**/hAT_2-M138A; lane 12, ^{125}I-**14**/hAT_2-M138A; lane 13, ^{125}I-**13**/hAT_2-M128,138A; lane 14, ^{125}I-**14**/hAT_2-M128,138A; lane 15, ^{125}I-**13** + ^{125}I-**14**/Mock. Prestained broad-range protein standards were run in parallel. Each AngII analogue−hAT_2 receptor interaction was specific and decreased in a dose-dependent manner in the presence of AngII (results not shown). The means ± SE are shown for five independent experiments.

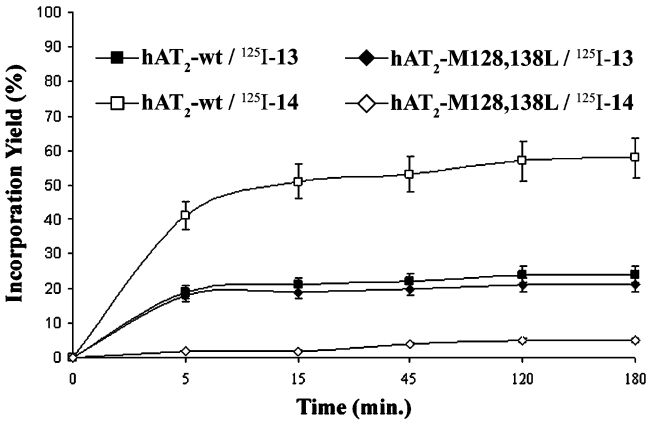

Figure 5. Time-course experiments of the incorporation yields of ^{125}I-**13** and ^{125}I-**14** on the hAT_2-wt and isosteric hAT_2-M128,138L double-mutant receptors. Receptor-transfected cell membranes were photolabeled for 5−180 min with either ^{125}I-**13** or ^{125}I-**14**, solubilized, and analyzed by 7.5% Tris−glycine/SDS−PAGE followed by autoradiography (see the Experimental Section for details). Each AngII analogue−hAT_2 receptor interaction was specific and decreased in a dose-dependent manner in the presence of AngII (results not shown). The means ± SE are shown for five independent experiments.

incorporation yield of all the model receptors. A systematic study of photoalkylation of amino acids by benzophenone showed that Met was the preferred target.[58] In fact, efficient hydrogen abstraction by Bpa only occurs from benzylic positions or from α-CH to heteroatoms.[15] Obviously, for both **12** and Bpa, some chemical selectivity may arise from steric constraints and from the chemical nature of the surrounding residues.

Conclusions

The herein presented synthetic access to Fmoc-**12** will undoubtedly increase its heretofor quite limited use in receptor photoaffinity labeling studies. Compared to biradical ketone-generating Bpa, carbene-generating **12** shows an absence of Met selectivity and an improved incorporation yield into unreactive residues of GPCRs. Given that the TMDs of GPCRs are extremely rich in residues containing inert aliphatic side chains, this difference in reactivity and chemical selectivity of both **12** and Bpa is of particular importance since the absence of methionine in the binding pocket of a receptor (e.g., hAT_2-M128,138A) can result in apparent failure to photolabel sufficiently through a ligand containing the benzophenone labeling moiety. Bpa will however maintain its importance since it allows rapid determination of the ligand−receptor contact point when used in scanning approaches such as MPA.[22,23] The different photolabeling properties of both photoprobes are the main reasons why photolabeling of the same membrane receptor with different photoprobes has led to contradictory results and conclusions. Keeping in mind that an ideal photoprobe should efficiently photolabel residues in its immediate contact, regardless of the chemical nature of these residues, it is of importance to have access to several complementary photoprobes.

Experimental Section

Chemistry. Starting materials and reagents were from Sigma-Aldrich Canada Ltd. and were used without further purification unless otherwise specified. Solvents, hydrochloric acid, acetic acid, *tert*-butyl alcohol, iodine, sodium hydroxide, and silver nitrate were from Fisher Scientific Ltd. Tris(dibenzylideneacetone)dipalladium-(0) was from Alfa Aesar. *N*-[(9-Fluorenyl)methoxycarbonyloxy]-succinimide and Wang resin (*p*-benzyloxybenzyl alcohol resin) were from Novabiochem (EMD Biosciences). IODO-GEN iodination reagent (1,3,4,6-tetrachloro-3α,6α-diphenylglycoluril) was from Pierce Biotechnology Inc. Na^{125}I was from Perkin-Elmer Canada Inc. Solvents were distilled and dried in a nitrogen atmosphere according to standard procedures.[59] *n*-Butyllithium (1.6 M solution in *n*-hexanes) was titrated according to the standard procedure.[60] All reactions requiring anhydrous conditions were conducted under a positive argon atmosphere in vacuumed flame-dried glassware using standard syringe techniques. Analytical thin-layer chromatography (TLC) was carried out on precoated (0.25 mm) Merck silica gel 60f-254 plates. Flash chromatography was performed on Merck silica gel 60 (230−400 mesh) using air pressure according to the standard procedure.[61] Spots were detected by fluorescence quenching at 254 or 350 nm, treating with iodine and/or a revealing solution (sulfuric acid−molybdic acid, cerium ammonium nitrate, or potassium permanganate−potassium carbonate), and heating. Reversed-phase high-pressure liquid chromatography (RP-HPLC) purification was performed using a Waters 625 LC instrument equipped with a Waters C-18 reversed-phase column monitored by absorbance at 214 nm as well as by a γ-radioisotope detector. NMR spectra were obtained using a Bruker AC-300 instrument (300 MHz). Chemical shifts are reported in δ values (ppm) relative to the peak for chloroform (300 MHz adjusted to 7.26 ppm for ^{1}H NMR and 62.5 MHz adjusted to 77.0 ppm for ^{13}C NMR) as an internal standard. Coupling constants (*J*) are in hertz. The following abbreviations were used for the NMR spectra assignments: s = singlet; d = doublet; t = triplet; q = quartet; m = multiplet. The melting points of crystalline compounds were determined using a Büchi M-50 apparatus and are uncorrected. Optical rotations were measured using a Perkin-Elmer 141 polarimeter at the sodium D line (589 nm) with a 10.00 cm and 1.0 mL cell. The mass spectra of amino acid derivatives were obtained using a VG Micromass ZAB-2F instrument with electronic ionization (70 eV) and of peptides using a Tofspec2 Micromass instrument with matrix-assisted laser desorption ionization time of flight (MALDI-TOF). Last, photoreactive diazirine derivatives were handled in dim yellow light in flasks covered with aluminum foil.

3-(*p*-Iodophenyl)-3-(trifluoromethyl)diaziridine (5).[37,38] Compound **5** was synthesized in four steps starting from **1** according to the literature.[37,38]

***N*-[(9-Fluorenyl)methoxycarbonyl]-L-serine (7).**[41] Compound **7** was synthesized in one step starting from **6** according to the literature.[41]

***N*-[(9-Fluorenyl)methoxycarbonyl]-L-serine *tert*-Butyl Ester (8).**[42] Dicyclohexylcarbodiimide (680 mg, 3.3 mol equiv), *tert*-butyl alcohol (401 μL, 4.2 mol equiv), and copper(I) chloride (7 mg, 0.07 mol equiv) were placed in an argon-purged, three-necked, round-bottom flask fitted with a magnetic stirrer and a condenser. The suspension was stirred at room temperature for 72 h until the reaction had ended as judged by TLC (ethyl acetate (3)/petroleum ether (7)). The dark green suspension was diluted in anhydrous methylene chloride (2.0 mL, 0.5 M final), and compound **7** (327

mg, 1.0 mol equiv) was added. The resulting suspension was purged with argon and was stirred at room temperature for 2 h until the reaction had ended as judged by TLC (ethyl acetate (3)/petroleum ether (7)). The reaction mixture was filtered, and the white dicyclohexylurea precipitate was washed with methylene chloride (2 × 2 mL). The filtrate was combined with the reaction mixture, which was diluted with ethyl acetate (6 mL). The organic layer was washed with a saturated $CaCO_3$ solution (12 mL) and brine (2 × 12 mL). The ethyl acetate/methylene chloride solution was dried over anhydrous magnesium sulfate, vacuum filtered, and evaporated under reduced pressure. The crude product was purified by flash chromatography on silica gel using ethyl acetate/methylene chloride as an eluant, leaving pure compound **8** as a white crystalline solid. Yield: 67% (257 mg). Mp: 122−123 °C. ^{1}H NMR ($CDCl_3$, 300 MHz, δ (ppm)): 7.77 (d, J = 7.4 Hz, 2H, $H_{4,5}$-Fmoc), 7.61 (d, J = 7.4 Hz, 2H, $H_{1,8}$-Fmoc), 7.41 (t, J = 7.4 Hz, 2H, $H_{3,6}$-Fmoc), 7.32 (t, J = 7.4 Hz, 2H, $H_{2,7}$-Fmoc), 5.68 (d, J = 6.6 Hz, 1H, N*H*), 4.42 (d, J = 7.0 Hz, 2H, O−CH_2-Fmoc), 4.33 (m, 1H, α-C*H*), 4.23 (t, J = 6.9 Hz, 1H, C*H*-Fmoc), 3.94 (m, 2H, β-CH_2), 2.51 (s, O-*H*), 1.49 (s, 9H, *t*-Bu).

***N*-[(9-Fluorenyl)methoxycarbonyl)]-L-(*β*-iodo)alanine *tert*-Butyl Ester (9). First Protocol**.[43] Compound **8** (383 mg, 1.0 mol equiv), methyltriphenoxyphosphonium iodide (497 mg, 1.1 mol equiv), and anhydrous *N*,*N*-dimethylformamide (2.0 mL, 0.5 M final) were placed in an argon-purged round-bottom flask fitted with a magnetic stirrer. The resulting solution was stirred at room temperature for 1 h until the reaction had ended as judged by TLC (ethyl acetate (3.0)/petroleum ether (7.0)). The reaction mixture was diluted with ethyl acetate (4 mL), and the organic layer was washed with distilled water (6 mL), a saturated sodium thiosulfate solution (6 mL), and a saturated $CaCO_3$ solution (6 mL). The ethyl acetate solution was dried over anhydrous magnesium sulfate, vacuum filtered, and evaporated under reduced pressure. The crude product was purified by flash chromatography on silica gel using ethyl acetate/methylene chloride as an eluant, leaving pure compound **9** as a slightly yellow crystalline solid. Yield: 88% (434 mg). Mp: 81−83 °C. ^{1}H NMR ($CDCl_3$, 300 MHz, δ (ppm)): 7.77 (d, J = 7.4 Hz, 2H, $H_{4,5}$-Fmoc), 7.62 (d, J = 7.4 Hz, 2H, $H_{1,8}$-Fmoc), 7.41 (t, J = 7.1 Hz, 2H, $H_{3,6}$-Fmoc), 7.33 (tt, J = 7.4, 1.6 Hz, 2H, $H_{2,7}$-Fmoc), 5.69 (d, J = 7.1 Hz, 1H, N*H*), 4.46−4.32 (m, 3H, α-C*H* + OCH_2-Fmoc), 4.25 (t, 1H, J = 7.1 Hz, C*H*-Fmoc), 3.61 (d, J = 3.4 Hz, 2H, β-CH_2), 1.53 (s, 9H, *t*-Bu).

Second Protocol.[44] Compound **8** (383 mg, 1.0 mol equiv) and anhydrous methylene chloride (2.0 mL, 0.5 M final) were placed in an argon-purged round-bottom flask fitted with a magnetic stirrer. In the following order, chlorodiphenylphosphine (269 μL, 1.5 mol equiv), imidazole (102 mg, 1.5 mol equiv), and iodine (380 mg, 1.5 mol equiv) were then added. The suspension was purged with argon and was stirred at room temperature for 1 h until the reaction had ended as judged by TLC (ethyl acetate(4.5)/*n*-hexanes (5.0)/acetic acid (0.5)). The reaction mixture was diluted with methylene chloride (4 mL), and the organic layer was washed with distilled water (6 mL), a saturated sodium thiosulfate solution (6 mL), and a saturated $CaCO_3$ solution (6 mL). The methylene chloride solution was dried over anhydrous magnesium sulfate, vacuum filtered, and evaporated under reduced pressure. The crude product was purified by flash chromatography on silica gel using ethyl acetate/methylene chloride as an eluant, leaving pure compound **9** as a slightly yellow crystalline solid. Yield: 53% (261 mg).

***N*-[(9-Fluorenyl)methoxycarbonyl)]-*p*-[3-(trifluoromethyl)-diaziridine]-L-phenylalanine *tert*-Butyl Ester (10).**[45] Zinc dust (325 mesh; 196 mg, 3.0 mol equiv), chlorotrimethylsilane (64 μL, 0.5 mol equiv), and anhydrous *N*,*N*-dimethylformamide (400 μL, resulting in a 7.5 M solution) were placed in an argon-purged, flame-dried, round-bottom flask fitted with a magnetic stirrer. The suspension was vigorously stirred at room temperature for 30 min. The stirring was stopped to let the Zn* decant for 1 h. The chlorotrimethylsilane and *N*,*N*-dimethylformamide were then removed using a syringe. A solution of compound **9** (493 mg, 1.0 mol equiv) in anhydrous *N*,*N*-dimethylformamide (0.5 mL, 2.0 M final) was added dropwise to the activated anhydrous Zn*. The resulting suspension was stirred at room temperature for 30 min until the reaction had ended as judged by TLC (ethyl acetate (2)/petroleum ether (8)). Compound **5** (314 mg, 1.0 mol equiv), the catalyst tris(dibenzylideneacetone)dipalladium(0) (27 mg, 0.03 mol equiv), and the ligand tri-*o*-tolylphosphine (47 mg, 0.15 mol equiv) were quickly added to the Zn−**9** suspension. The mixture was purged with argon and stirred at room temperature for 1 h until the reaction had ended as judged by TLC (ethyl acetate (2)/*n*-hexanes (8)). The reaction mixture was filtered through a Celite pad from which the Zn* was washed with ethyl acetate (3 × 3 mL). The filtrate was combined with the reaction mixture, and the organic layer was washed with a saturated sodium thiosulfate solution (2 × 9 mL) and brine (2 × 9 mL). The ethyl acetate solution was dried over anhydrous magnesium sulfate, vacuum filtered, and evaporated under reduced pressure. The crude product was purified by flash chromatography on silica gel using ethyl acetate/petroleum ether as an eluant, leaving pure compound **10** as a dark red oil. Yield: 55% (304 mg). Mp: 88−89 °C. ^{1}H NMR ($CDCl_3$, 350 MHz, δ (ppm)): 7.77 (d, J = 7.5 Hz, 2H, $H_{4,5}$-Fmoc), 7.55 (m, 4H, $H_{1,8}$-Fmoc + *m*-*H*), 7.41 (t, J = 7.3 Hz, 2H, $H_{3,6}$-Fmoc), 7.31 (t, J = 7.3 Hz, 2H, $H_{2,7}$-Fmoc), 7.20 (d, J = 7.4 Hz, 2H, *o*-*H*), 5.29 (d, J = 7.8 Hz, 1H, N*H*), 4.55 (∼q, J = 6.4 Hz, 1H, α-C*H*), 4.47 (td, J = 8.8, 2.0 Hz, 1H, OC*H*H-Fmoc), 4.34 (t, J = 8.7 Hz, 1H, OCH*H*-Fmoc), 4.20 (t, 1H, J = 6.8 Hz, C*H*-Fmoc), 3.12 (d, J = 5.6 Hz, 2H, β-CH_2), 2.78 (d, J = 8.0 Hz, 1H, N*H*−NH), 2.16 (d, J = 9.0 Hz, 1H, NH−N*H*), 1.40 (s, 9H, *t*-Bu).

***N*-[(9-Fluorenyl)methoxycarbonyl]-*p*-[3-(trifluoromethyl)-3*H*-diazirin-3-yl]-L-phenylalanine *tert*-Butyl Ester (11).**[38,39] Compound **10** (554 mg, 1.0 mol equiv), freshly prepared silver oxide (see below; 1.16 g, 5.0 mol equiv), and diethyl ether (4.0 mL, 0.25 M final concentration) were placed in a round-bottom flask fitted with a magnetic stirrer and a condenser. The suspension was stirred at room temperature for 8 h in the dark until the reaction had ended as judged by TLC (ethyl acetate (3)/petroleum ether (7)). The reaction mixture was diluted with diethyl ether (4 mL), dried over anhydrous magnesium sulfate, and filtered through a Celite pad to remove the silver, silver oxide, and magnesium sulfate, which were washed with diethyl ether (3 × 8 mL). The filtrate was combined with the reaction mixture, and the diethyl ether solution was evaporated under reduced pressure, leaving crude **11** as a red oil, which was used for the last step without further purification. The compound may be further purified by flash chromatography on silica gel using ethyl acetate/petroleum ether as an eluant to obtain pure product compound **11** as a white crystalline solid. Yield: 87%. Mp: 85−86 °C. ^{1}H NMR ($CDCl_3$, 350 MHz, δ (ppm)): 7.78 (d, J = 7.5 Hz, 2H, $H_{4,5}$-Fmoc), 7.58 (dd, 2H, J = 1.7, 0.8 Hz, $H_{1,8}$-Fmoc), 7.42 (t, J = 7.4 Hz, 2H, $H_{3,6}$-Fmoc), 7.32 (td, J = 7.4, 1.1 Hz, 2H, $H_{2,7}$-Fmoc), 7.12 (dd, J = 19.8, 8.3 Hz, 4H, *m*-*H* + *o*-*H*), 5.41 (d, J = 7.9 Hz, 1H, N*H*), 4.50 (m, 2H, α-C*H* + OC*H*H-Fmoc), 4.35 (∼t, J = 8.7 Hz, 1H, OCH*H*-Fmoc), 4.20 (t, J = 6.8 Hz, 1H, C*H*-Fmoc), 3.10 (d, J = 5.9 Hz, 2H, β-CH_2), 1.40 (s, 9H, *t*-Bu).

Silver Oxide Solution. A 1 M solution of sodium hydroxide (13 mL, 1.1 mol equiv) was added dropwise to a 1 M boiling solution of silver nitrate (2.0 g, 1.0 mol equiv) with stirring. The precipitated silver oxide was filtered, washed with distilled water (15.0 mL), acetone (15.0 mL), and diethyl ether (15.0 mL), and used immediately.

***N*-[(9-Fluorenyl)methoxycarbonyl]-*p*-[3-(trifluoromethyl)-3*H*-diazirin-3-yl]-L-phenylalanine (Fmoc-12)**.[45] Compound **11** (552 mg, 1.0 mol equiv), methylene chloride (10.0 mL, 0.1 M final), triethylsilane (242 μL, 1.5 mol equiv), and α,α,α-trifluoroacetic acid (3.9 mL, 50.0 mol equiv, ∼40% (v/v)) were placed in a round-bottom flask fitted with a magnetic stirrer and a condenser. The solution was stirred at room temperature for 3 h until the reaction had ended as judged by TLC (ethyl acetate (1.0)/methylene chloride (8.9)/acetic acid (0.1)). The reaction mixture was washed with water (2 × 10 mL) and brine (2 × 10 mL). The methylene chloride solution was dried over anhydrous magnesium sulfate, vacuum filtered, and evaporated under reduced pressure. The crude product was purified by flash chromatography on silica gel using ethyl acetate (1.0)/methylene chloride (8.9)/acetic acid (0.1) as an eluant,

leaving pure compound Fmoc-**12** as a white crystalline solid. An alternative purification method involves the precipitation of the compound dissolved in a minimum volume of methylene chloride at room temperature by the addition of petroleum ether at 0 °C with vigorous stirring followed by filtration. Yield: 81% (397 mg). Mp: 129−130 °C. $[\alpha]^{25}_{D}$ (c = 1.06, $CHCl_3$): +36.70. ^{1}H NMR ($CDCl_3$, 350 MHz, δ (ppm)): 7.78 (d, J = 7.6 Hz, 2H, $H_{4,5}$-Fmoc), 7.55 (d, J = 7.1 Hz, 2H, $H_{1,8}$-Fmoc), 7.42 (t, J = 7.3 Hz, 2H, $H_{3,6}$-Fmoc), 7.30 (td, J = 7.4, 1.1 Hz, 2H, $H_{2,7}$-Fmoc), 7.11 (q, J = 8.3 Hz, 4H, *m-H* + *o-H*), 5.16 (d, J = 8.0 Hz, 1H, N*H*), 4.68 (q, J = 7.5 Hz, 1H, α-C*H*), 4.51 (∼t, J = 8.7 Hz, 1H, OC*H*H-Fmoc), 4.40 (∼t, J = 8.7 Hz, 1H, OCH*H*-Fmoc), 4.20 (∼t, J = 6.5 Hz, 1H, C*H*-Fmoc), 3.17 (ddd, J = 21.0, 13.8, 5.6 Hz, 2H, β-CH_2). ^{13}C NMR ($CDCl_3$, 75 MHz, δ (ppm)): 174.75, 155.61, 143.63, 141.35, 137.30, 129.82, 127.80, 127.07, 126.64, 124.93, 120.04, 66.93, 54.22, 47.11, 37.21, 33.76, 31.98. EI-HRMS: *m/z* calcd for $C_{26}H_{20}N_3O_4F_3$ $[M + H]^+$ 495.1406, found $[M + H]^+$ 495.1397 ± 0.0015.

^{125}I[Sar[1],Tdf[8]]AngII (^{125}I-13).[46,47] Compound **12** was synthesized using the standard solid-phase peptide synthesis method with *N*-[(9-fluorenyl)methoxycarbonyl] (Fmoc)-protected amino acids and Wang resin (*p*-benzyloxybenzyl alcohol resin). Once the synthesis was completed and the side chain protecting group and resin linker were simultaneously cleaved, crude compound **13** was purified by RP-HPLC and was eluted as a single signal with a minimum of 95% purity. Compound **13** was characterized by MALDI-TOF-LRMS analysis as previously described[46] and showed *m/z* 1097 $[M + H]^+$ (*m/z* calcd for [Sar[1],Tdf[8]]AngII $[M + H]^+$ 1097). The resulting photoreactive peptides were radioiodinated using the IODO-GEN (1,3,4,6-tetrachloro-3α,6α-diphenylglycoluril) iodination method as described elsewere[62] and as previously described[47] to form radiophotoreactive ^{125}I-**13**. In brief, in the following order, 50 mM sodium phosphate buffer (pH 5.0, 30.0 μL, 20 mM final), 10^{-3} M AngII analogue (10 μL, 1.0 mol equiv), and 45 μM (5 mCi) Na^{125}I (10.0 μL, 1 mCi, 0.045 mol equiv) were added to an Eppendorf tube coated with IODO-GEN (20.0 μg, 4.6 mol equiv) in a final volume of 50.0 μL. The solution was incubated at room temperature for 15 min in the dark. The reaction conditions were optimized to form monoiodinated AngII analogues. The reaction mixture was quenched by adding a 50 mM sodium phosphate solution (50.0 μL) and incubated for a further 15 min. The radioiodinated AngII analogues were purified by RP-HPLC with a 20−40% acetonitrile gradient in 0.05% aqueous α,α,α-trifluoroacetic acid. The specific radioactivity of the labeled peptides was approximately 1500 Ci/mmol as determined by self-displacement and saturation binding analyses.[63]

^{125}I[Sar[1],Bpa[8]]AngII (^{125}I-14). Compound ^{125}I-**14** was synthesized, purified, and characterized as previously described.[46,47]

Biochemistry. Oligodeoxynucleotides, bovine serum albumin (BSA), bacitracin, and all other organic chemicals were from Sigma-Aldrich Ltd. All inorganic chemicals were from Fisher Scientific Ltd. pcDNA3.1 plasmid was from Invitrogen Inc. Site-directed mutagenesis materials, FuGENE 6 transfection reagent, Nonidet P-40, and Complete Protease Inhibitor Cocktail were from Roche Diagnostics. Cell culture materials and ^{14}C-labeled low molecular mass protein standards were from Gibco BRL. Electrophoresis materials and prestained broad-range protein standards were from Bio-Rad Laboratories Ltd. X-ray films (BioMaxMR) were from Kodak. Binding filters (1.0 μm grade GF/B glass microfiber, Whatman) were from VWR International Inc.

Oligodeoxynucleotide Site-Directed Mutagenesis. Site-directed mutagenesis was performed on the hAT_2-wt receptor with the overlap extension PCR method essentially as previously described.[64] Briefly, mutant receptors were subcloned into the *Hin*dIII−*Xba*I sites of the mammalian expression vector pcDNA3.1. Site-directed mutations were then confirmed by automated DNA sequencing.

Cell Culture and Transfections. COS-7 cells were grown in 10.0 mL of Dulbecco's modified Eagle's medium (DMEM) containing 2 mM L-glutamine, 10% (v/v) fetal bovine serum (FBS), 100 IU/mL penicillin, and 100 μg/mL streptomycin. The cells were seeded into 100 mm diameter culture dishes and incubated at 37 °C in a 5% CO_2 atmosphere until the density reached 6×10^6 cells/dish. Following trypsinization, 1.2×10^6 cells were suspended in a final volume of 10.0 mL of the same medium and grown for 24 h. The transfection conditions were performed according to the manufacturer's instructions. Briefly, the cells were transitorily transfected by adding a solution of FuGENE6 transfection reagent (6 μL) and plasmid DNA (3 μg) in 300 μL of serum-free DMEM, all of which had been previously incubated for 30 min at room temperature. Transfected cells were grown for an additional 36 h at 37 °C in a 5% CO_2 atmosphere. The cells were washed once with phosphate-buffered saline (PBS; 137 mM NaCl, 0.9 mM $MgCl_2$, 3.5 mM KCl, 0.9 mM $CaCl_2$, 8.7 mM Na_2HPO_4, and 3.5 mM NaH_2PO_4) and immediately stored at −80 °C until use.

Saturation Binding Assays. Cell membrane preparations and saturation binding assays were performed essentially as previously described.[65] Frozen transfected COS-7 cells were rapidly thawed for 1 min at 37 °C in a water bath, and 10.0 mL of ice-cold washing buffer (5 mM $MgCl_2$, 25 mM Trizma-Base, 100 mM NaCl; adjusted to pH 7.4) was added to the broken cells. The cells were gently scraped and centrifuged (500*g* for 15 min at 4 °C). The cell pellet was resuspended in 12.5 mL of ice-cold binding buffer (5 mM $MgCl_2$, 25 mM Trizma-Base, 100 mM NaCl, 0.1% (w/v) bovine serum albumin (BSA), and 0.01% (w/v) bacitracin; adjusted to pH 7.4), and 40 × 300 μL of the cell membrane suspension (20−40 μg of protein) was independently incubated in the dark for 60 min at room temperature with 100.0 μL of eight different final concentrations ranging from 5 nM (cell membrane suspensions 1−5) to 39 pM (cell membrane suspensions 36−40) of radioactive AngII analogues diluted to 100 Ci/mmol. To each of these eight final concentrations of radioactive AngII analogues were added binding buffer (3 × 100 μL; total binding) and AngII (5×10^{-6} M, 2 × 100 μL; nonspecific binding) for a final volume of 500 μL. Bound radioactive AngII analogue was separated from free radioactive AngII analogue by vacuum filtration through filters presoaked in binding buffer for 30 min at 0 °C. The radioactivity was evaluated by γ-radiation counting. A protein standard curve was used to determine cellular expression levels (B_{max}). The binding curves were analyzed for affinity (K_d) using the Ligand program.[66]

Photoaffinity Labeling Experiments. Cell membrane preparations and photoaffinity labeling experiments were performed essentially as previously described.[65] Frozen transfected COS-7 cells were rapidly thawed for 1 min at 37 °C in a water bath, and 10.0 mL of ice-cold washing buffer (5 mM $MgCl_2$, 25 mM Trizma-Base, and 100 mM NaCl; adjusted to pH 7.4) was added to the broken cells. The cells were then gently scraped and centrifuged (500*g* for 15 min at 4 °C). The cell pellet was resuspended in 500 μL of ice-cold binding buffer (5 mM $MgCl_2$, 25 mM Trizma-Base, 100 mM NaCl, 0.1% (w/v) bovine serum albumin (BSA), and 0.01% (w/v) bacitracin; adjusted to pH 7.4). The cell membrane suspension (800 μg to 1.6 mg of protein) was incubated in the dark for 60 min at room temperature in the presence of 10^7 cpm of radioactive AngII analogues (∼1500 Ci/mmol). The cell membranes were centrifuged (500*g* for 15 min at 4 °C). The pellet was resuspended in 500.0 μL of ice-cold washing buffer and irradiated for 5, 15, 45, 60, 120, or 180 min on ice under filtered UV light (365 nm; mercury vapor lamp JC-Par-38, no. 5873, Westinghouse and Raymaster black light filters, Gates and Co. Inc.). The cell membranes were centrifuged (2500*g* for 15 min at 4 °C), and the pellet was solubilized for 1 h on ice in modified radioimmunoprecipitation buffer (mRIPA buffer; 0.1% (w/v) SDS (electrophoresis grade), 0.25% (w/v) sodium deoxycholate, 1% (v/v) Nonidet P-40, 5 mM NaN_3, 50 mM Trizma−HCl (pH 7.4), and 150 mM NaCl) supplemented with Complete Protease Inhibitor Cocktail. The cell lysate was centrifuged (2500*g* for 30 min at 4 °C) to remove insoluble materials, and the supernatant was stored at −80 °C until use.

Incorporation Yield and Incorporation Yield Time-Course Experiments. The solubilized labeled proteins were diluted with Laemmli loading buffer (final concentration: 0.1% (w/v) bromophenol blue, 2% (w/v) SDS, 10% (v/v) glycerol, 50 mM Trizma−HCl (pH 6.8), and 100 mM dithiothreitol (DTT)) and incubated

for 1 h at 37 °C. Tris−glycine/SDS−polyacrylamide gel electrophoresis (SDS−PAGE) was performed essentially as described elsewere[67] using 7.5% analytical gels. Running conditions and gel fixation procedures were performed according to the manufacturer's instructions. To localize the labeled proteins (80−200 kDa), the dried gel was exposed to an X-ray film with an intensifying screen. Prestained broad-range protein standards were used to determine the apparent molecular masses (M_r). The incorporation yield of specific binding was calculated as follows on the same cell membrane preparations: [photolabeled receptor/ligand complex from Tris−glycine/SDS−PAGE (cpm)]/[specific binding (cpm)] × 100%. The specific activities of the radioiodinated AngII analogues did not have to be taken into account in the calculation since the photoaffinity labeling experiments to determine the value of photolabeled receptor/ligand complex from Tris−glycine/SDS−PAGE (cpm) and the saturation binding assay to determine the value of specific binding (cpm) were performed using either compound ^{125}I-**13** or compound ^{125}I-**14**.

Partial Purification of the Photolabeled Receptor/Radioligand Complex. Partial purification of the photolabeled receptor/radioligand complex was performed essentially as previously described.[65] The solubilized labeled proteins were diluted with Laemmli loading buffer (final concentration: 0.1% (w/v) bromophenol blue, 2% (w/v) SDS, 10% (v/v) glycerol, 50 mM Trizma−HCl (pH 6.8), and 100 mM DTT) and incubated for 1 h at 37 °C. Tris−glycine/SDS−PAGE was performed essentially as described elsewere[67] using 7.5% preparative gels. Running conditions and gel fixation procedures were performed according to the manufacturer's instructions. To localize the labeled proteins (80−200 kDa), the gel was exposed to an X-ray film with an intensifying screen. Prestained broad-range protein standards were used to determine the apparent molecular masses (M_r). Radioactive bands were excised from the gel, and the gel slices were macerated in 10 mL of the same buffer for 4 days at 4 °C with gentle agitation as described elsewere.[68] The macerated gel slices were centrifuged (2500*g* for 15 min at 4 °C), the supernatant containing the eluted labeled proteins was filtered (0.22 μm), and the whole filtrate was concentrated ∼100 times to a final volume of ∼100 μL. The partially purified photolabeled receptor/radioligand complex was aliquoted and was stored at −80 °C until use. Under these conditions, we repeatedly recovered at least 80% of the initial radioactivity.

C-Terminal Met-Specific CNBr Cleavage. The partially purified photolabeled receptor/radioligand complex (5000−10000 cpm, 10 μL) was diluted for a final concentration of 70% (v/v) formic acid (88% (v/v), 80 μL), and a solution of CNBr (5 mg) diluted in acetonitrile (10 μL) was added for a final volume of 100 μL. The resulting solution was incubated at room temperature for 18 h in the dark. The reaction mixture was quenched by adding H_2O (1 mL). The CNBr reaction mixture was lyophilized for 24 h. The lyophilizate was diluted in Laemmli loading buffer (final concentration: 0.1% (w/v) bromophenol blue, 2% (w/v) SDS, 10% (v/v) glycerol, 50 mM Trizma−HCl (pH 6.8), and 100 mM DTT) and was incubated for 5 min at ∼100 °C. Tris−Tricine/SDS−PAGE was performed essentially as described elsewere[69] using 16.5% T/3% C analytical gels. Running conditions and gel fixation procedures were performed according to the manufacturer's instructions. To localize the labeled proteins, the dried gel was exposed to an X-ray film with an intensifying screen. ^{14}C-labeled low molecular mass protein standards were used to determine the apparent molecular masses (M_r).

Acknowledgment. We are grateful to Marie-Reine Lefebvre for her expert help and technical assistance for peptide synthesis and to Dr. Pierre Deslongchamps for access to his facilities. This work was supported by the Canadian Institutes of Health Research. E.E. is a recipient of the J.C. Edwards Chair in Cardiovascular Research. This paper was submitted to fulfill the requirements of a Ph.D. thesis for D.F. at the Université de Sherbrooke.

Supporting Information Available: ^{1}H NMR, ^{13}C NMR, and EI-HRMS data for **12** as well as RP-HPLC and MALDI-TOF LRMS data for compounds **13** and **14**. This material is available free of charge via the Internet at http://pubs.acs.org.

References

(1) Kristiansen, K. Molecular mechanisms of ligand binding, signaling, and regulation within the superfamily of G-protein-coupled receptors: molecular modeling and mutagenesis approaches to receptor structure and function. *Pharmacol. Ther.* **2004**, *103*, 21−80.
(2) Wess, J. Structure−Function Analysis of G Protein-Coupled Receptors. In *Receptor Biochemistry and Methodology Series*; Sibley, D. R., Ed.; John Wiley & Sons: New York, 1999; p 432.
(3) Jahn, O.; Eckart, K.; Tezval, H.; Spiess, J. Characterization of peptide−protein interactions using photoaffinity labeling and LC/MS. *Anal. Bioanal. Chem.* **2004**, *378*, 1031−1036.
(4) Bayley, H. Photogenerated Reagents in Biochemistry and Molecular Biology. In *Laboratory Techniques in Biochemistry and Molecular Biology*; Work, T. S., Burdon, R. H., Eds.; Elsevier: Amsterdam/New York/Oxford, 1983; p 188.
(5) Brunner, J. Photochemical labeling of apolar phase of membranes. *Methods Enzymol.* **1989**, *172*, 628−687.
(6) Brunner, J. New photolabeling and crosslinking methods. *Annu. Rev. Biochem.* **1993**, *62*, 483−514.
(7) Kotzyba-Hibert, F.; Kapfer, I.; Goeldner, M. Recent trends in photoaffinity labeling. *Angew. Chem., Int. Ed. Engl.* **1995**, *34*, 1296−1312.
(8) Becker, O. M.; Shacham, S.; Marantz, Y.; Noiman, S. Modeling the 3D structure of GPCRs: advances and application to drug discovery. *Curr. Opin. Drug Discovery Dev.* **2003**, *6*, 353−361.
(9) Shacham, S.; Marantz, Y.; Bar-Haim, S.; Kalid, O.; Warshaviak, D.; et al. PREDICT modeling and in-silico screening for G-protein coupled receptors. *Proteins* **2004**, *57*, 51−86.
(10) Dorman, G. Photoaffinity labeling in biological signal transduction. *Top. Curr. Chem.* **2000**, *211*, 169−225.
(11) Dorman, G.; Prestwich, G. D. Using photolabile ligands in drug discovery and development. *Trends Biotechnol.* **2000**, *18*, 64−77.
(12) Hatanaka, Y.; Sadakane, Y. Photoaffinity labeling in drug discovery and developments: chemical gateway for entering proteomic frontier. *Curr. Top. Med. Chem.* **2002**, *2*, 271−288.
(13) Kauer, J. C.; Erickson-Viitanen, S.; Wolfe, H. R., Jr.; DeGrado, W. F. p-Benzoyl-L-phenylalanine, a new photoreactive amino acid. Photolabeling of calmodulin with a synthetic calmodulin-binding peptide. *J. Biol. Chem.* **1986**, *261*, 10695−10700.
(14) Dorman, G.; Prestwich, G. D. Benzophenone photophores in biochemistry. *Biochemistry* **1994**, *33*, 5661−5673.
(15) Prestwich, G. D.; Dorman, G.; Elliott, J. T.; Marecak, D. M.; Chaudhary, A. Benzophenone photoprobes for phosphoinositides, peptides and drugs. *Photochem. Photobiol.* **1997**, *65*, 222−234.
(16) Laporte, S. A.; Boucard, A. A.; Servant, G.; Guillemette, G.; Leduc, R.; et al. Determination of peptide contact points in the human angiotensin II type I receptor (AT1) with photosensitive analogs of angiotensin II. *Mol. Endocrinol.* **1999**, *13*, 578−586.
(17) Kage, R.; Leeman, S. E.; Krause, J. E.; Costello, C. E.; Boyd, N. D. Identification of methionine as the site of covalent attachment of a p-benzoyl-phenylalanine-containing analogue of substance P on the substance P (NK-1) receptor. *J. Bio.l Chem.* **1996**, *271*, 25797−25800.
(18) Bisello, A.; Adams, A. E.; Mierke, D. F.; Pellegrini, M.; Rosenblatt, M.; et al. Parathyroid hormone-receptor interactions identified directly by photocross-linking and molecular modeling studies. *J. Biol. Chem.* **1998**, *273*, 22498−22505.
(19) Behar, V.; Bisello, A.; Rosenblatt, M.; Chorev, M. Direct identification of two contact sites for parathyroid hormone (PTH) in the novel PTH-2 receptor using photoaffinity cross-linking. *Endocrinology* **1999**, *140*, 4251−4261.
(20) Behar, V.; Bisello, A.; Bitan, G.; Rosenblatt, M.; Chorev, M. Photoaffinity cross-linking identifies differences in the interactions of an agonist and an antagonist with the parathyroid hormone/parathyroid hormone-related protein receptor. *J. Biol. Chem.* **2000**, *275*, 9−17.
(21) Macdonald, D.; Mierke, D. F.; Li, H.; Pellegrini, M.; Sachais, B.; et al. Photoaffinity labeling of mutant neurokinin-1 receptors reveals additional structural features of the substance P/NK-1 receptor complex. *Biochemistry* **2001**, *40*, 2530−2539.
(22) Rihakova, L.; Deraet, M.; Auger-Messier, M.; Perodin, J.; Boucard, A. A.; et al. Methionine proximity assay, a novel method for exploring peptide ligand−receptor interaction. *J. Recept. Signal Transduction Res.* **2002**, *22*, 297−313.

(23) Clement, M.; Martin, S. S.; Beaulieu, M. E.; Chamberland, C.; Lavigne, P.; et al. Determining the environment of the ligand binding pocket of the human angiotensin II type I (hAT1) receptor using the methionine proximity assay. *J. Biol. Chem.* **2005**, *280*, 27121−27129.
(24) Fleming, S. A. Chemical reagents in photoaffinity labeling. *Tetrahedron* **1995**, *51*, 12479−12520.
(25) Borden, W. T.; Gritsan, N. P.; Hadad, C. M.; Karney, W. L.; Kemnitz, C. R.; et al. The interplay of theory and experiment in the study of phenylnitrene. *Acc. Chem. Res.* **2000**, *33*, 765−771.
(26) Hatanaka, Y.; Nakayama, H.; Kanaoka, Y. Diazirine-based photoaffinity labeling: chemical approach to biological interfaces. *Rev. Heteroat. Chem.* **1996**, *14*, 213−243.
(27) Nassal, M. 4′-(1-Azi-2,2,2-trifluoroethyl)phenylalanine, a photolabile carbene-generating analogue of phenylalanine. *J. Am. Chem. Soc.* **1984**, *106*, 7540−7545.
(28) Shih, L. B.; Bayley, H. A carbene-yielding amino acid for incorporation into peptide photoaffinity reagents. *Anal. Biochem.* **1985**, *144*, 132−141.
(29) Fishwick, C. W. G.; Sanderson, J. M.; Findlay, J. An efficient route to S-N-(9-fluorenylmethoxycarbonyl)-4′-(1-azi-2,2,2-trifluoroethyl)-phenylalanine. *Tetrahedron Lett.* **1994**, *35*, 4611−4614.
(30) Hashimoto, M.; Hatanaka, Y.; Sadakane, Y.; Nabeta, K. Synthesis of tag introducible (3-trifluoromethyl)phenyldiazirine based photoreactive phenylalanine. *Bioorg. Med. Chem. Lett.* **2002**, *12*, 2507−2510.
(31) Servant, G.; Laporte, S. A.; Leduc, R.; Escher, E.; Guillemette, G. Identification of angiotensin II-binding domains in the rat AT2 receptor with photolabile angiotensin analogs. *J. Biol. Chem.* **1997**, *272*, 8653−8659.
(32) Servant, G.; Dudley, D. T.; Escher, E.; Guillemette, G. Analysis of the role of N-glycosylation in cell-surface expression and binding properties of angiotensin II type-2 receptor of rat pheochromocytoma cells. *Biochem. J.* **1996**, *313* (Part 1), 297−304.
(33) Diez, J. Angiotensin II and the hypertensive heart: a role for the AT2 receptor? *J. Hypertens.* **2004**, *22*, 879−882.
(34) Unger, T. The angiotensin type 2 receptor: variations on an enigmatic theme. *J. Hypertens.* **1999**, *17*, 1775−1786.
(35) Nouet, S.; Nahmias, C. Signal transduction from the angiotensin II AT2 receptor. *Trends Endocrinol. Metab.* **2000**, *11*, 1−6.
(36) de Gasparo, M.; Siragy, H. M. The AT2 receptor: fact, fancy and fantasy. *Regul. Pept.* **1999**, *81*, 11−24.
(37) Jensen, B. J.; Hergenrother, P. M.; Nwokogu, G. Poly(arylene ether)s with pendant ethynyl groups. *J. Macromol. Sci., Pure Appl. Chem.* **1993**, *A30*, 449−458.
(38) Topin, A. N.; Gritsenko, O. M.; Brevnov, M. G.; Gromova, E. S.; Korshunova, G. A. Synthesis of a new photo-cross-linking nucleoside analogue containing an aryl(trifluoromethyl)diazirine group: application for E*co*RII and M*ua*I restriction-modification enzymes. *Nucleosides Nucleotides* **1998**, *17*, 1163−1175.
(39) Nassal, M. 4-(1-Azi-2,2,2-trifluoroethyl)benzoic acid, a highly photolabile carbene generating label readily fixable to biochemical agents. *Liebigs Ann. Chem.* **1983**, 1510−1523.
(40) Brunner, J.; Spiess, M.; Aggeler, R.; Huber, P.; Semenza, G. Hydrophobic labeling of a single leaflet of the human erythrocyte membrane. *Biochemistry* **1983**, *22*, 3812−3820.
(41) Blaskovich, M. A.; Lajoie, G. A. Synthesis of a chiral serine aldehyde equivalent and its conversion to chiral alpha-amino acid derivatives. *J. Am. Chem. Soc.* **1993**, *115*, 5021−5030.
(42) Schultz, M.; Kunz, H. Synthetic O-glycopeptides as model substrates for glycosyltransferases. *Tetrahedron: Asymmetry* **1993**, *4*, 1205−1220.
(43) Verheyden, J. P. H.; Moffatt, J. G. Halo sugar nucleosides. I. Iodination of the primary hydroxyl groups of nucleosides with methyltriphenoxyphosphonium iodide. *J. Org. Chem.* **1970**, *35*, 2319−2326.
(44) Classon, B.; Zhengchun, L. New halogenation reagent systems useful for the mild one-step conversion of alcohols into iodides or bromides. *J. Org. Chem.* **1988**, *53*, 6126−6130.
(45) Deboves, H. J. C.; Montalbetti, C. A. G. N.; Jackson, R. F. W. Direct synthesis of Fmoc-protected amino acids using organozinc chemistry: application to polymethoxylated phenylalanines and 4-oxoamino acids. *J. Chem. Soc., Perkin Trans. 1* **2001**, 1876−1884.
(46) Bosse, R.; Servant, G.; Zhou, L. M.; Boulay, G.; Guillemette, G.; et al. Sar1-p-benzoylphenylalanine-angiotensin, a new photoaffinity probe for selective labeling of the type 2 angiotensin receptor. *Regul. Pept.* **1993**, *44*, 215−223.
(47) Laporte, S. A.; Servant, G.; Richard, D. E.; Escher, E.; Guillemette, G.; et al. The tyrosine within the NPXnY motif of the human angiotensin II type 1 receptor is involved in mediating signal transduction but is not essential for internalization. *Mol. Pharmacol.* **1996**, *49*, 89−95.
(48) Munson, M.; Balasubramanian, S.; Fleming, K. G.; Nagi, A. D.; O'Brien, R.; et al. What makes a protein a protein? Hydrophobic core designs that specify stability and structural properties. *Protein Sci.* **1996**, *5*, 1584−1593.
(49) Sachon, E.; Bolbach, G.; Chassaing, G.; Lavielle, S.; Sagan, S. Cgamma H2 of Met174 side chain is the site of covalent attachment of a substance P analog photoactivable in position 5. *J. Biol. Chem.* **2002**, *277*, 50409−50414.
(50) Brunner, J.; Senn, H.; Richards, F. M. 3-Trifluoromethyl-3-phenyldiazirine. A new carbene generating group for photolabeling reagents. *J. Biol. Chem.* **1980**, *255*, 3313−3318.
(51) Weber, P. J.; Beck-Sickinger, A. G. Comparison of the photochemical behavior of four different photoactivatable probes. *J. Pept. Res.* **1997**, *49*, 375−383.
(52) Ploug, M. Identification of specific sites involved in ligand binding by photoaffinity labeling of the receptor for the urokinase-type plasminogen activator. Residues located at equivalent positions in uPAR domains I and III participate in the assembly of a composite ligand-binding site. *Biochemistry* **1998**, *37*, 16494−16505.
(53) Tate, J. J.; Persinger, J.; Bartholomew, B. Survey of four different photoreactive moieties for DNA photoaffinity labeling of yeast RNA polymerase III transcription complexes. *Nucleic Acids Res.* **1998**, *26*, 1421−1426.
(54) Gillingham, A. K.; Koumanov, F.; Hashimoto, F.; Holman, G. D. *Detection and Analysis of Glucose Transporters Using Photolabelling Techniques*; Oxfrod University Press: Oxford, 2000; p 193.
(55) Bobrowski, K.; Marciniak, B.; Hug, G. L. 4-Carboxybenzophenone-sensitized photooxidation of sulfur-containing amino acids. Nanosecond laser flash photolysis and pulse radiolysis studies. *J. Am. Chem. Soc.* **1992**, *114*, 10279−10288.
(56) Marciniak, B.; Bobrowski, K.; Hug, G. L. Quenching of triplet states of aromatic ketones by sulfur-containing amino acids in solution. Evidence for electron transfer. *J. Am. Chem. Soc.* **1993**, *97*, 11937−11943.
(57) Marciniak, B.; Hug, G. L.; Bobrowski, K.; Kozubek, H. Mechanism of 4-carboxybenzophenone-sensitized photooxidation of methionine-containing dipeptides and tripeptides in aqueous solution. *J. Phys. Chem.* **1995**, *99*, 13560−13568.
(58) Deseke, E.; Nakatami, Y.; Ourisson, G. Intrinsic reactivities of amino acids toward photoalkylation with benzophenone—a study preliminary to photolabelling of the transmembrane protein glycophorin A. *Eur. J. Org. Chem.* **1998**, *243*, 3−251.
(59) Armarego, W. L. F. *Purification of Laboratory Chemicals*, 4th ed.; Butterworth-Heinemann: Oxford, Boston, Johannesburg, Melbourne, New Delhi, Singapore, 1999; 529 pp.
(60) Bergbreiter, D. E.; Pendergrass, E. Analysis of organomagnesium and organolithium reagents using N-phenyl-1-naphthylamine. *J. Org. Chem.* **1981**, *46*, 219−220.
(61) Still, W. C.; Kahn, M.; Mitra, A. Rapid chromatographic technique for preparative separations with moderate resolution. *J. Org. Chem.* **1978**, *43*, 2923−2925.
(62) Fraker, P. J.; Speck, J. C., Jr. Protein and cell membrane iodinations with a sparingly soluble chloroamide, 1,3,4,6-tetrachloro-3a,6a-diphrenylglycoluril. *Biochem. Biophys. Res. Commun.* **1978**, *80*, 849−857.
(63) Wiener, H. L.; Reith, M. E. Determination of radioligand specific activity using competition binding assays. *Anal. Biochem.* **1992**, *207*, 58−62.
(64) Boucard, A. A.; Sauve, S. S.; Guillemette, G.; Escher, E.; Leduc, R. Photolabelling the rat urotensin II/GPR14 receptor identifies a ligand-binding site in the fourth transmembrane domain. *Biochem. J.* **2003**, *370*, 829−838.
(65) Boucard, A. A.; Wilkes, B. C.; Laporte, S. A.; Escher, E.; Guillemette, G.; et al. Photolabeling identifies position 172 of the human AT(1) receptor as a ligand contact point: receptor-bound angiotensin II adopts an extended structure. *Biochemistry* **2000**, *39*, 9662−9670.
(66) Munson, P. J.; Rodbard, D. Ligand: a versatile computerized approach for characterization of ligand-binding systems. *Anal. Biochem.* **1980**, *107*, 220−239.
(67) Laemmli, U. K. Cleavage of structural proteins during the assembly of the head of bacteriophage T4. *Nature* **1970**, *227*, 680−685.
(68) Blanton, M. P.; Cohen, J. B. Identifying the lipid−protein interface of the Torpedo nicotinic acetylcholine receptor: secondary structure implications. *Biochemistry* **1994**, *33*, 2859−2872.
(69) Schagger, H.; von Jagow, G. Tricine-sodium dodecyl sulfate-polyacrylamide gel electrophoresis for the separation of proteins in the range from 1 to 100 kDa. *Anal. Biochem.* **1987**, *166*, 368−379.

JM050958A